The heart of oxygenic photosynthesis illuminated

Janssen, G.J.

Chapter 6

Outlook

In this thesis new insights into the photochemical machinery of cyanobacterial and plant reaction centers have been presented. Through selective isotope labelling of cyanobacteria and plants, the primary ET events in PSI and PSII could be studied at the atomic level directly in whole cells or entire plants (see chapter 2 and 4). In this chapter we will provide perspectives on future studies with sparsely ^{13}C and ^{15}N labeled PSI and PSII protein complexes. In chapter 3 the functional flexibility and field dependence of PSI has been discussed based on data obtained from uniformly ^{15}N labeled PSI complex from different plant systems. The kinetics of the photo-CIDNP buildup presented in chapter 5 indicated that functional flexibility is an inherent property of PSI. In this chapter this discussion will be continued based on preliminary results obtained from 4-ALA ^{13}C labeled PSI complexes that were measured at different magnetic field strengths. In chapter 4 new evidence for the involvement of the protein matrix in ET in PSII RCs has been presented. In this chapter preliminary results obtained from ^{15}N-ALA labeled PSII will be presented that can further support the evidence for a histidine residue with some electron spin density ρ_i.

6.1 FIELD DEPENDANCE OF PHOTO-CIDNP BUILDUP

The magnetic field dependence of photo-CIDNP signals is a sensitive tool to study photo-CIDNP buildup mechanisms and investigate how the nuclear polarization depends on the magnetic parameters and on the lifetimes of the intermediate radical species (Jeschke 1997; Prakash *et al.* 2005). The field dependence of PSII and PSI has previously been studied by ^{13}C photo-CIDNP MAS NMR on unlabeled PSI and PSII preparations from spinach (Roy *et al.* 2007). PSII shows a field dependence similar to RCs of purple bacteria (Prakash *et al*. 2005), with maximum polarization at the lowest tested field of 4.7 T. In the meantime this trend has shown to extend to even lower fields of 2.35 T in PSII (data not shown), but due to the decrease in signal resolution the optimal field strength for PSII investigations remains 4.7 T. PSI of spinach on the other hand shows an optimal signal to noise ratio at 9.4 T (Roy *et al.* 2007). As discussed in chapter 3 of this thesis the same trend was found for PSI particles of duckweed based on a photo-CIDNP study of uniformly ^{15}N

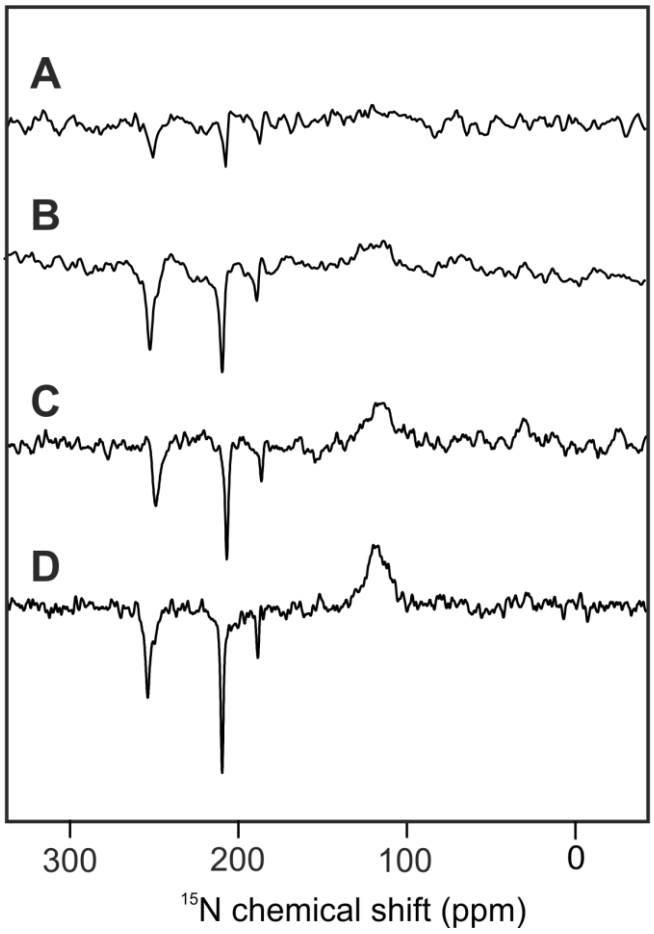

Figure 6.1 ^{15}N photo-CIDNP MAS NMR spectra obtained from the same pre-reduced sample of uniformly ^{15}N labeled PSI-110 particles of duckweed measured at magnetic field strengths of 2.35 T (A), 4.7 T (B), 7.1 T (C) and 9.4 T (D). All spectra have been obtained with a spinning frequency of 8 kHz, at a temperature of 235 K and with a recycle delay of 4 s. The light intensity was kept constant at 320 klux in all experiments. The number of scans was the same for the experiments that were performed at 235 K.

labeled PSI-110 particles. Figure 6.1 shows spectra obtained from uniformly ^{15}N labeled PSI-110 particles of duckweed and illustrates the increase in signal intensity observed upon increasing the magnetic field strength from 2.35 T to 9.4 T. As has been discussed in chapter 3, the field dependence observed for PSI confirms a different electronic structure for the radical pair compared to PSII and the bacterial RC. In addition, the data discussed in chapter 3 imply a functional flexibility of PSI in different plant species.

6.2 FUNCTIONAL FLEXIBILITY OF PSI

Figure 6.2 shows ^{13}C photo-CIDNP MAS NMR spectra obtained from selectively ^{13}C 4-ALA labeled PSI-110 particles from duckweed. Trace a shown in panel A of Figure 6.2 was collected by continuous illumination of a 4-ALA ^{13}C labeled PSI-110 complex

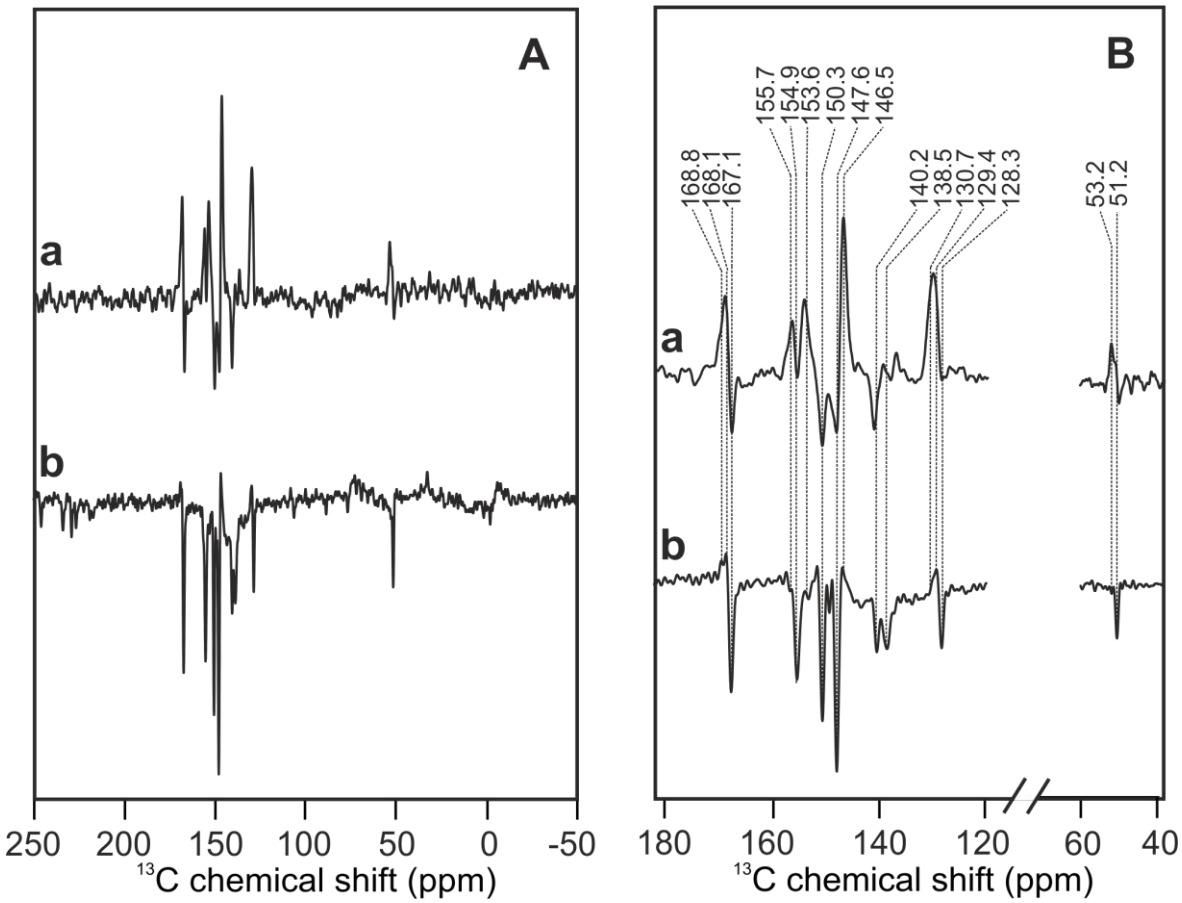

Figure 6.2: ^{13}C photo-CIDNP MAS NMR spectra obtained by continuous illumination of selectively ^{13}C 4-ALA labeled PSI-110 particles of duckweed at 4.7 T (a) and 9.4 T (b) at 235K and with a recycle delay of 4 s. Figure B shows the aromatic and aliphatic regions of spectra a and b in A in more detail, with the dashed lines indicating the centerbands of the observed light induced signals.

preparation, frozen directly inside the NMR probe in the dark while spinning slowly prior to NMR detection in a magnetic field of 4.7 T. Spectrum b in the left panel of Figure 6.2 was collected from a 4-ALA ^{13}C labeled PSI-110 in a magnetic field of 9.4 T. Figure 5.2B shows the aromatic and aliphatic regions with the light induced centerbands indicated by the dashed lines. The signal buildup for the isolated 4-ALA ^{13}C labeled PSI from duckweed was ~10 fold faster than the signal buildup in whole cells of cyanobacteria, and the signal to noise ratio was significantly improved (see chapter 2, Figure 2.3 and Figure 6.2). This is in agreement with the higher level of label incorporation in duckweed with P_{tot} = 75 ± 5 % as opposed to ~30 ± 5 % in cyanobacteria (See Appendix A and Figure 2.2, respectively) and the higher concentration of PSI RCs in preparations containing isolated PS-110 complexes as opposed to whole cells.

In Table 6.1, an overview is presented of the ^{13}C photo-CIDNP signals observed in the current work, and these results are compared with data from previous studies that were

Table 6.1: ^{13}C chemical shifts for photo-CIDNP signals obtained at 4.7 and 9.4 T, in comparison with literature data

Chemical shifts					
		n.a. Plant PSI	4-ALA Cyanobac PSI	4-ALA Plant PSI	
Chl *a*	assignment carbon atom	9.4 T	4.7 T	4.7 T	9.4 T
σ_{ss} [a]		σ [b]	σ [c]	σ [d]	σ [d]
170.0	**19**	167.1 e	166.9 e	168.3 a	168.8 a
				167.1 e	167.1 e
162.0	14	160.4 e			
155.9	**1**	154.8 e	154.8 e	153.6 a	154.9 e
154.4	**6**			155.7 a	
			149.8 e	150.3 e	150.3 e
154.0	16	152.6 e			
150.7	4	149.9 e			
147.2	**11**	147.2 e	147.6 e	146.5 a	146.5 a
147.2	9			147.6 e	147.6 e
146.2	**8**	144.2 e	144.2 e	140.7 e	140.2 e
138.0	**3**	138.6 e	138.6 e		138.5 e
136.1	2	~ 136 e			
134.0	12				
133.4	7	~ 132 e		129.8 a	130.7 a
					129.4 a
126.2	**13**		128.3 e		128.3 e
108.2	10	105.4 e	~ 104.5 e		
102.8	15				
98.1	5				
93.3	20				
51.4	**17**				51.2 e
				53.2 a	

[a] Boender *et al.* (1995), data obtained from solid aggregates of Chl *a*. [b]Alia *et al.* (2004), data obtained from isolated PSI particles from spinach. [c] data obtained from *Synechocytis* whole cells containing both PSI and PSII but showing pure PSI. [d] obtained from 4-ALA labeled isolated PSI from duckweed. Abbreviations: σ = chemical shift, a = absorptive signal, e = emissive signal

performed on a variety of PSI preparations from different organisms, at magnetic field strengths of 4.7 and 9.4 T. The chemical shifts of the positive features obtained from 4-ALA ^{13}C labeled PSI at 9.4 T match with the positive signals observed at 4.7 T (see Table 6.1). In earlier ^{13}C -photo-CIDNP studies on isolated PSI-110 particles from spinach, PSI has always shown a purely emissive spectrum (Alia *et al.* 2004; Diller *et al.* 2005). Likewise, as has been discussed in chapter 2, all signals assigned to PSI in the ^{13}C photo-CIDNP MAS NMR spectra obtained from whole cells of *Synechocystis* sp. PCC 6803 cyanobacteria were emissive. The similarity of the chemical shift patterns observed for the PSI of different organisms and at different experimental conditions, suggests that the electronic ground states

at the molecular level is largely species and preparation independent. The apparent changes in the signal intensity pattern confirm a large functional flexibility at the higher level of the protein complex, which depends both on the species and on the experimental conditions. PSII on the other hand shows little variation in both chemical shift and relative signal intensity pattern among different plant species, isolation states and experimental conditions (chapter 4 and Figure 5.6).

Upon prolonged illumination, *i.e.* an experimental time of more than ~20 h with continuous illumination at 235K, the positive features observed at 9.4 T (spectrum 6.2b) decrease in intensity (data not shown). On the other hand prolonged illumination at 4.7 T causes the negative signals shown in Figure 6.2a to diminish (data not shown). The same effect is observed in the data obtained from uniformly ^{15}N labeled PSI complex. Here the absorptive peaks observed in PSI samples from duckweed disappear upon prolonged illumination (see Figure 3.3A of freshly reduced PSI and Figure 6.1B of pre-reduced PSI for comparison). In addition, similar to the observations in cyanobacteria at 4.7 T (see Figure 2.5 page 48), the signal buildup rate for the emissive photo-CIDNP signals at 9.4 T increases upon prolonged illumination of isolated PSI complex from duckweed (data not shown). Further systematic experimentation has to be performed to quantify and understand the observed changes in the photo-CIDNP spectra of PSI upon prolonged illumination. Possible explanations for the light induced changes and the strong field dependence include (i) a change in the relative contribution of the TSM and DD mechanisms in the photo-CIDNP buildup or (ii) a change in the relative activity of the two cofactor branches in PSI ET at different conditions.

In PSI both cofactor branches are active in ET (Fairclough *et al.* 2003; Ramesh *et al.* 2004; Poluektov *et al.* 2005; Santabarbara *et al.* 2005; Santabarbara *et al.* 2010). Upon illumination the PSI forms radical pairs with the electron donor P700 as the radical cation and either the A_{0A} or A_{0B} Chl *a* cofactor as radical anion. The two radical pairs ($P700^{+\bullet}A_{0A}^{-\bullet}$ and $P700^{+\bullet}A_{0B}^{-\bullet}$) are generated in a pure singlet state and the initial electronic zero-quantum coherence is converted by the TSM and DD mechanisms into net nuclear polarization. The TSM mechanism breaks the symmetry of the coherent spin evolution in the correlated radical pair by state mixing due to anisotropic electron-electron dipolar coupling and pseudosecular hyperfine coupling. Coherence transfer is maximal when the difference of the electron Zeeman frequencies $\Delta\Omega$, the nuclear Zeeman frequency ω_I, and the secular part of the hyperfine interaction (A) fulfill the double matching condition $2|\Delta\Omega| = 2|\omega_I| = |A|$

(Jeschke, 1997, 1998; Jeschke and Matysik, 2003). In the DD mechanism the symmetry is broken due to the different lifetimes of the singlet and triplet radical pair state and the pseudosecular hyperfine coupling (Polenova and McDermott, 1999). For the DD mechanism only a single matching of conditions is required: $2|\omega_I| = |A|$ and the difference of the singlet and triplet radical pair lifetimes should be in the order of the inverse hyperfine coupling (Jeschke and Matysik, 2003). Since both $\Delta\Omega$ and $\underline{\omega_I}$ depend on the magnetic field, both the TSM and DD mechanisms produce the highest absolute nuclear polarization at a matching field but can generate polarization with opposite signs (Roy *et al.* 2007). Based on quantum chemistry calculations and the time-resolved data obtained from uniformly labeled PSI-110 particles discussed in chapter 5, section 3, it can be concluded that in PSI the DD mechanism is dominant. Previous simulations indicated an increase of the exchange coupling *J* between the $P700^{+\bullet}$ and $A_0^{-\bullet}$ radical anions by a factor of approximately 3 opposed to the bacterial RC, which can explain the field effect observed in PSI (Jeschke and Matysik 2003; Roy *et al.* 2007, Stoll and Schweiger 2006). It was suggested that the change in *J*-coupling arises from minor rearrangements of the cofactors, leading to a larger overlap between the molecular orbitals of the P700 donor and the accessory Chl *a* or between the molecular orbitals of the accessory Chl *a* and the primary acceptor A_0. A change in the *J*-coupling has a strong effect on the field dependence via the matching condition for Photo-CIDNP (Jeschke and Matysik 2003). While the local protein environment of the A_{0A} and A_{0B} Chl *a* cofactors and their relative orientation to the P700 donor are very similar (Jordan *et al.* 2001), the cation is mainly localized on P_B (Davis *et al.* 1993; Käss *et al.* 2001, Saito and Ishikita 2011). This could affect the relative strength of the exchange coupling between A_{0A} and A_{0B} to P_B and the optimal field for the observation of either the A_{0A} or A_{0B} electron acceptor.

The relative activity of the A and B branch depend on the organism and the reduction state of the quinone A_{1A} (Ali *et al.* 2006). In plants and green algae the A:B branch activity is about 50:50 but upon photo-accumulation of A_{1A}^- due to the complete reduction of the F_X cluster, the relative contribution of the B branch increases and becomes dominant (Santabarbara *et al.* 2006). In cyanobacteria a similar trend is visible, yet buildup of the contribution of the B branch takes longer and the resulting signal is weak with a maximum relative activity of 55 to 60% (Santabarbara *et al.* 2005 and 2006, Poluektov *et al.* 2005). As discussed in chapter 5 the conditions during our photo-CIDNP experiments result in a relatively slow F_X reduction with a gradual increase in the fraction of the $P700^{+\bullet}A_0^{-\bullet}$ radical pair during the experiment. This explains why upon continuous illumination of PSI during

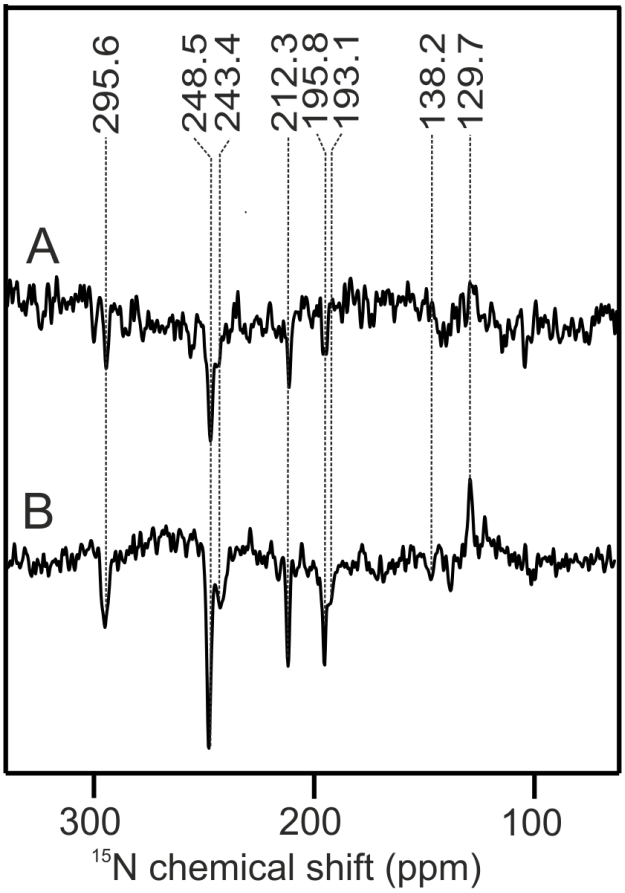

Figure 6.3 ^{15}N photo-CIDNP MAS NMR spectra obtained from ^{15}N-ALA labeled thylakoid (A), and uniformly ^{15}N labeled isolated PSII D1D2 complex from duckweed (B). Both spectra were measured at a magnetic field strength of 4.7 T and have been obtained with a spinning frequency of 8 kHz, a temperature of 235 K and a recycle delay of 4 s.

the NMR measurement the rate of signal buildup increases. In addition it provides a possible explanation for the observed light induced changes observed in cyanobacteria and duckweed. Full reduction of F_X causes the relative activity of the B branch to increase strongly while the participation of the A branch in ET decreases (Santabarbara *et al.* 2006). As noted before this alteration in the relative branch activity upon prolonged illumination is expected to be stronger in plants than in cyanobacteria (Poluektov *et al.* 2005; Santabarbara *et al.* 2006). This is in line with the pronounced light induced changes observed in the photo-CIDNP spectra obtained from duckweed plants (Figure 6.2) and the minor changes observed for *Synechocyctis* cyanobacteria (Figure 2.5, page 48).

6.3 ^{15}N PHOTO-CIDNP MAS NMR ON ^{15}N LABELED PSII

The signals at 136.0 and 132.0 ppm in the ^{13}C photo-CIDNP MAS NMR spectra obtained from PSII complexes with ^{13}C at natural abundance (see Figure 4.4B) provides

Table 6.2: ^{15}N chemical shifts of the photo-CIDNP signals obtained from ^{15}N-ALA labeled PSII in comparison to signals obtained from uniformly ^{15}N-labeled PSII and literature data

Assignment		Solution data	u-^{15}N PSII spinach	u-^{15}N PSII duckweed	^{15}N-ALA duckweed
cofactor	atom	σ^{a}_{LS}	$\sigma_{SS}{}^{b}$	$\sigma_{SS}{}^{c}$	$\sigma_{SS}{}^{c}$
Chl *a*	N-I	186.0		193.1 e	
	N-II	206.5	211.5 e	212.3 e	212.3 e
	N-III	189.4	195.3 e	195.8 e	195.8 e
	N-IV	247.0	247.6 e	248.5 e	248.5 e
Phe *a*	N-I	125.5		129.7 a	
	N-II	241.5		243.4 e	243.4 e
	N-III	133.9	138.3 e	138.2 e	
	N-IV	295.8	295.0 e	295.6 e	295.6 e

[a] Chl *a* and Phe *a* in $CDCl_2$, chemical shifts in ppm. Boxer *et al.* 1974.

[b] Uniformly ^{15}N labeled PSII D1D2 complex from spinach, chemical shifts in ppm. Diller *et al.* 2007.

[c] Uniformly ^{15}N labeled PSII D1D2 complex and ^{15}N-ALA labeled thylakoid from duckweed, chemical shifts in ppm. Abbreviations: σ = chemical shift, a = absorptive signal, e = emissive signal, u-^{15}N = uniformly ^{15}N labeled.

further support for a histidine residue with some spin density ρ_i in close proximity to the Chl *a* donor P_{D1} of PSII (Matysik *et al.* 2001; Diller *et al.* 2005). In this natural abundance spectrum not only ρ_i carrying carbons from the Chl *a* and Phe *a* cofactors appear. as is the case in selectively 3-, 4-, and 5-ALA ^{13}C labeled preparations but also ρ_i carrying carbons from the surrounding protein matrix will appear. Recently it has been suggested that a (B)Chl$^{\delta-}$-His$^{\delta+}$ partial charge transfer motif is a common denominator across photosynthetic RC complexes in plants and bacteria and that this interaction can help to establish a dynamic polaron mechanism for barrier-less electron transfer in photosynthetic complexes (Alia *et al.* 2013, Eisenmayer *et al.* 2012). Experiments with selectively ^{15}N-ALA label patterns would be of great interest to facilitate a final conclusion regarding the involvement of protein side chains as electron spin carriers in PSII. Figure 6.3A shows the preliminary results of ^{15}N photo-CIDNP MAS NMR applied to ^{15}N-ALA labeled thylakoid from duckweed. The quality of the data has to be further improved for final conclusions but a first comparison with data obtained from uniformly labeled ^{15}N PSII is still possible (Figure 6.3B). If ρ_i is located on a nitrogen atom of the protein matrix surrounding the RC cofactors, the corresponding photo-CIDNP signal will appear in the data collected from uniformly labeled PSII, and not in the data obtained from ^{15}N-ALA labeled PSII. The signals at 138.2 and

193.1 ppm in Figure 6.3 are weak and are difficult to resolve from the noise background in the data collected from ^{15}N-ALA labeled PSII. However, the sharp absorptive peak appearing at 129.7 ppm in the spectrum obtained from uniformly ^{15}N labeled PSII is interesting (Figure 6.3A). This is the only absorptive signal in Figure 6.3A and is very weak or absent in the spectrum obtained from ^{15}N-ALA labeled PSII (Figure 6.3B, Table 6.2). Based on the chemical shift the signal at 129.7 ppm can in principle be assigned to the N-I nitrogen of the Phe *a* acceptor (cf. Table 6.2). However, considering the relative strength of the 129.7 ppm signal in Figure 6.3B, it would be expected to be visible in Figure 6.3A as well, if it indeed originates from a nitrogen atom of the Phe *a* cofactor. Calculations using the TZP basis and the SAOP model have delivered reliable predictions for chemical shift and signal intensity patterns in PSI photo-CIDNP NMR spectra (see chapter 5 and Appendix B). Preliminary calculations using a similar approach for PSII provide no indication for sign reversal of the signal originating from the N-I of the Phe *a* donor in line with a different origin of the absorptive signal at 129.7 ppm. Further improvement of the spectral data from ^{15}N-ALA labeled PSII is required to arrive at a final conclusion on this point.

6.4 TIME-RESOLVED PHOTO-CIDNP EXPERIMENTS ON LABELED PSII

While continuous illumination spectra of 3, 4 and 5-ALA ^{13}C labeled duckweed PSII spectra are readily available (chapter 4), attempts to obtain reliable time-resolved ns-flash photo-CIDNP data of selectively ^{13}C labeled PSII in thylakoid, BBY and whole plants samples have consistently failed because of the high sensitivity of PSII to intense laser flashes. Due to the high cost of the ^{13}C-ALA precursor required for the preparation of labeled PSII, it was not possible to prepare a sufficient amount of selectively ^{13}C labeled D1D2 to compensate for the rapid degradation of the PSII activity for thylakoid, BBY and plant samples, which occurred even when the laser power was reduced to 80 mJ, compared with ~200 mJ in experiments on bacterial RC and PSI. The necessity to reduce the quinones in thylakoid, BBY and whole plant samples, causes additional sensitization of the already fragile PSII complex. Natural repair mechanisms which have shown to partly regenerate PSII activity in core preparations upon dark incubation after illumination at 4 °C or at room temperature, fail to function in the presence of sodium dithionite reductant (Braun *et al.* 1990). Hence further research to stabilize PSII during laser experiments is necessary. PSII from the cyanobacterial species *Thermococcus* (*T.*) *vulcanus* (Kamiya and Shen 2003), which is extremely stable (Hughes *et al.* 2010) might be a suitable candidate for additional

laser studies. As discussed in chapter 2 of this thesis, selective ^{13}C isotope labeling was successfull for *Synechocystis* sp. PCC 6803 cyanobacteria, and the closely related *T. vulcanus* may be a promising candidate for selective isotope labeling.

6.5 THE APPLICATION OF 2D AND 3D NMR EXPERIMENTS TO LABELED PSI AND PSII

As discussed in paragraph 5.3, quantum chemical calculations are very useful in assigning the photo-CIDNP MAS NMR response from PSI (using the TZP basis and SAOP model potential for best results, Bode *et al.* manuscript in preparation, appendix B) and the same procedure can be applied to PSII. In addition it is possible to apply 3D transferred-echo double resonance (TEDOR) (Jaroniec *et al.* 2002, Hing *et al.* 1992, Helmus *et al.* 2011) and frequency selective rotational-echo double-resonance (REDOR) (Jaroniec *et al.* 2001) MAS NMR to PSI an PSII samples which are both uniformly ^{15}N and selectively ^{13}C labeled. 3D TEDOR allows for the simultaneous measurement of multiple carbon-nitrogen distances in ^{13}C,^{15}N-labeled solids by ^{13}C-^{15}N coherence transfer and ^{15}N and ^{13}C frequency labeling for site-specific resolution while the detrimental effects of homonuclear ^{13}C-^{13}C *J*-couplings on the measurement of weak ^{13}C-^{15}N dipolar couplings are circumvented (Jaroniec *et al.* 2002). Through these experiments the signal assignment would be simplified due to the information that is encoded in the carbon-nitrogen couplings. This is relevant because the ^{15}N signals arising in PSII from the Chl *a* donor and Phe acceptor are well resolved, while the carbon spectra show considerable signal overlap also for the spectra obtained from selectively ^{13}C labeled samples. Frequency selective REDOR allows for the recoupling of a single ^{13}C-^{15}N dipolar interaction in a multiple spin system, while all remaining ^{13}C-^{15}N dipolar couplings and ^{13}C-^{13}C scalar couplings to the selected ^{13}C are suppressed. In this way local structural distortions of the cofactors can be probed like *e.g.* the involvement of the axial histidine, His-198, in the stabilization of the HOMO on P_{D1} in PSII (Diller 2008, Diller *et al.* 2007).